CHAPTER 3

MATERIALS AND EXPERIMENTAL METHODS

The most important characteristics of a catalyst for soot oxidation are its activity, selectivity and stability. To obtain reliable and meaningful results, catalysts need to be designed with utmost care. Experimental conditions must be adjusted so that the intrinsic activity of the catalyst is measured, free from the effect of mass and heat transfer. Determination of catalytic activity is closely associated with the development of catalysts for new processes or improved formulation for practical application. New catalysts are usually tested on a relatively small scale before putting them to a large scale. Therefore, bench scale tubular reactor has been used in this study for the measurement of the catalytic activity and for carrying out the kinetic studies.

3.1 Materials Required

Locally available commercial diesel (HP) and AR grade chemicals such as Citric acid, Urea, Na_2CO_3, $PdCl_2$, $La(NO_3)_3.6H_2O$, $Fe(NO_3)_3.9H_2O$, $Ni(NO_3)_2$, $Zn(NO_3)_2.6H_2O$, $Cu(NO_3)_2 \cdot 3H_2O$, $Co(NO_3)_2.6H_2O$, $Sr(NO_3)_2$, etc. were used in the present research work.

3.2 Synthesis of Catalysts

The following methods were used for the preparation of perovskite catalysts:

1. Co-precipitation Method;

2. Citric acid Sol-gel Method;

3. Combustion Synthesis Method;

4. Reactive Grinding Method.

3.2.1 Co-precipitation (Co-ppt) Method

Co-precipitation method is the simplest and most widely used for the preparation of perovskite catalysts [Wang et al. 2007]. Synthesis of perovskite is by co-precipitation of soluble salts of the constituent metals in a suitable solvent and then co-precipitated by adding an acid/base or other reagent to cause the precipitation. These can be readily converted to oxides by thermal treatments. Precipitation has three stages: super saturation, nucleation, and growth. An amorphous or crystalline precipitate or a gel is obtained which is aged, filtered, washed thoroughly until salt free. This is then followed by further steps: drying, shaping, calcination, and activation. Various characterization techniques confirmed that the co-precipitation method produces lower crystallinity and higher surface area than other methods. In addition, the final material obtained from the alkali co-precipitation route suffers from the contamination of alkaline metals as well as the formation of a large amount of environmental wastes (e.g., salts from hydrolysis and wash water). Figure 3.1 shows the flow diagram of catalyst preparation by co-precipitation method.

A typical co-precipitation method used by Dhakad et al. [2008] to synthesize $SrCoO_3$ type perovskite catalyst is described as follows: nitrate salts of strontium and cobalt are mixed together in aqueous solution and stirred for 15 min with heating. About 300 ml of 0.5 N KOH and 1 M ammonium carbonate solutions then slowly add

to the above metal solutions at a rate of 50 ml/min with constant stirring. The precipitate thus obtained is allowed to settle overnight followed by filtration with thorough washings with de-ionized water. The precipitate cake is kept in an oven at 80◦C for drying and the resultant mass is then calcined at 650^{o}C for 4 h followed by grinding and further calcination at 950^{o}C for 8 h.

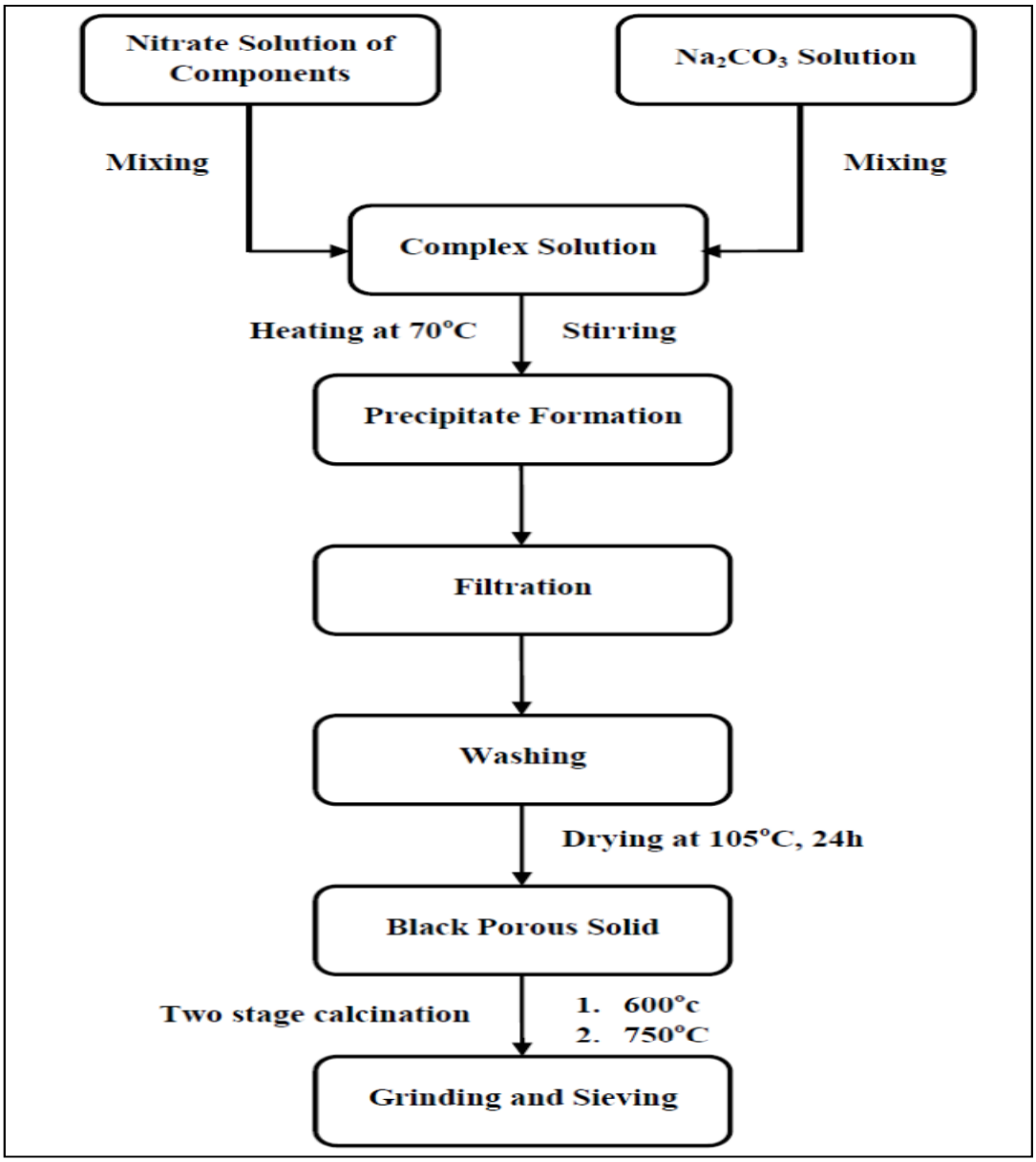

Figure 3.1 Schematic diagram for preparation of perovskite catalyst by co-precipitation method

3.2.2 Citric Acid Sol-gel (SG) Method

Perovskite catalysts are prepared by a citrate sol-gel method as follows: the reagents (nitrate salts of desired oxides) first dissolve in distilled water in stoichiometric amounts. A given amount of citric acid dissolved in deionized water is added in above solution as a ligand [Li et al. 2012, Wang et al. 2012]. The solution is adjusted to pH=7.5-8.0 with aqueous ammonia or acetic acid, stirring and heating to a temperature of 60-80^{o}C for 4 h, syrup obtained is then heated to 100^{o}C for 24 h in air, followed by calcination at 450◦C for 2 h, and then temperature is raised to 600^{o}C in 4 h. Black samples are obtained [Lopez-Surez et al. 2009, Wu et al 2009]. This method is the most effective route to create high surface area catalysts [Li et al. 2010, Wang et al. 2011]. A typical example of $La_{o.9}K_{o.1}CoO_3$ prepared by the sol-gel method is given by Wang et al. [2006]. Analytical grade $La(NO_3)_3.H_2O$, KNO_3 and $Co(NO_3)_2.6H_2O$ are weighed according to the stoichiometric ratio, and then dissolved in distilled water. Some citric acid is added with the same mole fraction as for the metallic ions. The mixture is stirred for 3 h while ammonia is added to adjust the pH value to be 8-9. The mixture is dehydrated by placing in a water bath at 80-90^{o}C. The sample slowly becomes sol, and then gels. After being heat-treated at 120^{o}C for 2 h, the sample is put into an oven at a temperature of 300-400^{o}C for 4 h, and the sample becomes powder. The powder is kept at 500^{o}C for 2 h after being further ground. Then it is calcined at 800^{o}C for 12-24 h, thus the $La_{o.9}K_{o.1}CoO_3$ perovskite composite oxide is obtained. Figure 3.2 shows the flow diagram of catalyst preparation by sol-gel method.

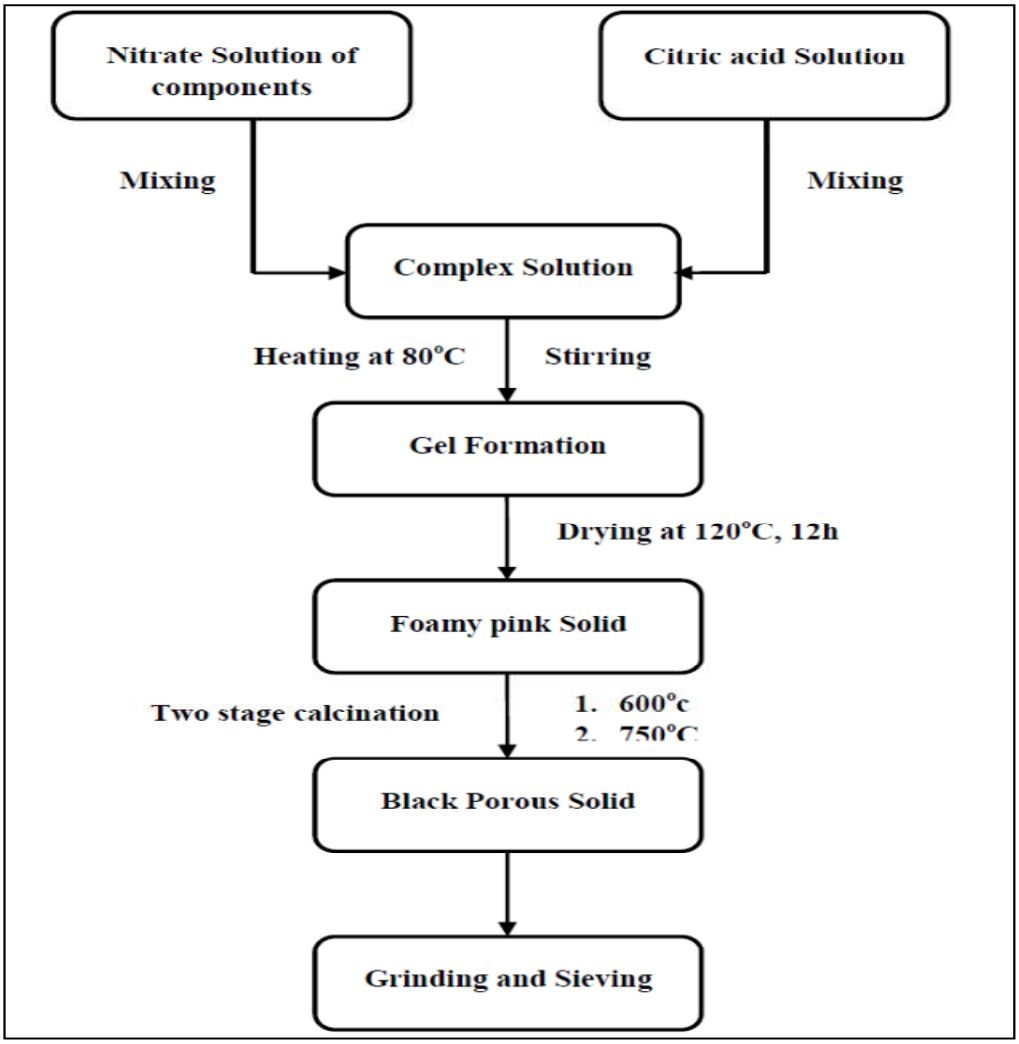

Figure 3.2 Flow diagram of Sol-gel method

3.2.3 Solution Combustion Synthesis (SCS)

Combustion synthesis was carried out starting from a homogeneous water solution containing metal nitrates as precursors of the desired oxide and urea as sacrificial fuel [Biamino et al. 2005]. The synthesis process can be formally split into two steps. The first one is endothermic and represents the real perovskite synthesis starting from the metal nitrate precursors, while the second is exothermic and accounts for the reaction between oxygen derived from nitrates decomposition and urea. Some direct combustion of urea with atmospheric oxygen cannot of course be excluded as the preparation is carried out in air (Fino et al. 2003, Fino et al. 2006]. The catalysts are then calcined in

air at 500^{o}C for 4 h to burn the carbonaceous matters as a common stabilization treatment [Russo et al. 2008]. Taking the $LaCrO_3$ synthesis as an example, the combustion synthesis involving lanthanum nitrate, chromium nitrate and urea occurs according to the following overall reaction (3.1) which gives rise to a perovskite powder and gaseous species:

$$\mathbf{La(NO_3)_3 + Cr(NO_3)_3 + 5CO(NH_2)_2 \longrightarrow LaCrO_3 + 5CO_2 + 8N_2 + 10H_2O} \quad (3.1)$$

The whole reaction can be formally regarded as the combination of two different contributions:

$$\mathbf{La(NO_3)_3 + Cr(NO_3)_3 \longrightarrow LaCrO_3 + 7.5O_2 + 3N_2} \quad \textbf{(endothermic)} \quad (3.2)$$

$$\mathbf{5CO(NH_2)_2 + 7.5O_2 \longrightarrow 5CO_2 + 10H_2O + 5N_2} \quad \textbf{(exothermic)} \quad (3.3)$$

The exothermic reaction (3.3), namely urea combustion, provides the heat that is necessary for the completion of the decomposition reaction (3.2), i.e., the endothermic transformation of nitrate into the desired oxide (Biamino and Badini 2004, Ifrah et al. 2007]. This technique is particularly suited for the production of nano-sized particles of catalyst [Russo et al. 2005]. The whole process is carried out in a pot, therefore it is also known as a single pot synthesis technique. Figure 3.3 shows the flow diagram of SCS method.

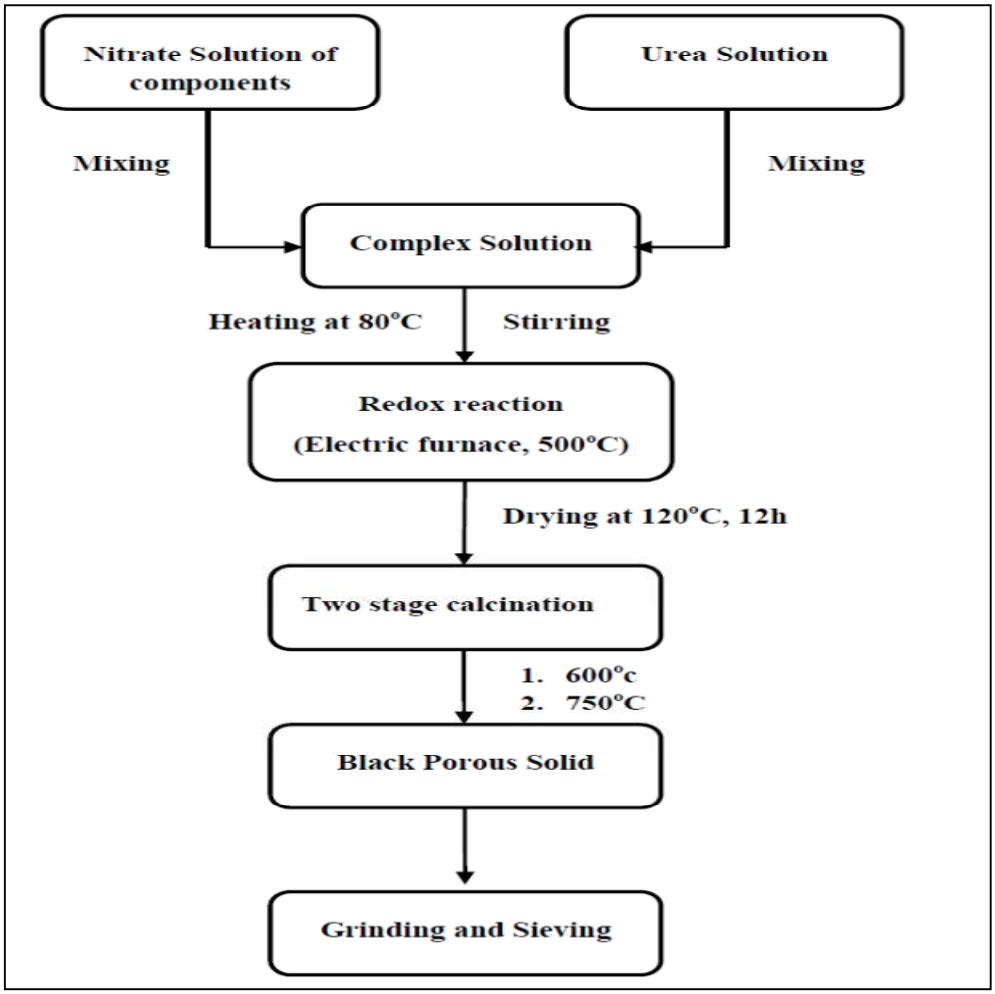

Figure 3.3 Flow diagram of SCS method

Simultaneous TGA/DTA analyses are used for investigating the mechanism of combustion synthesis process as shown in Figure 3.4 for a typical $LaCrO_3$ [Biamino and Badini 2004]. The irregular shape of the exothermal peak in the DTA curve for the three component system reveals that the combustion synthesis occurs in a complex way, involving several reactions.

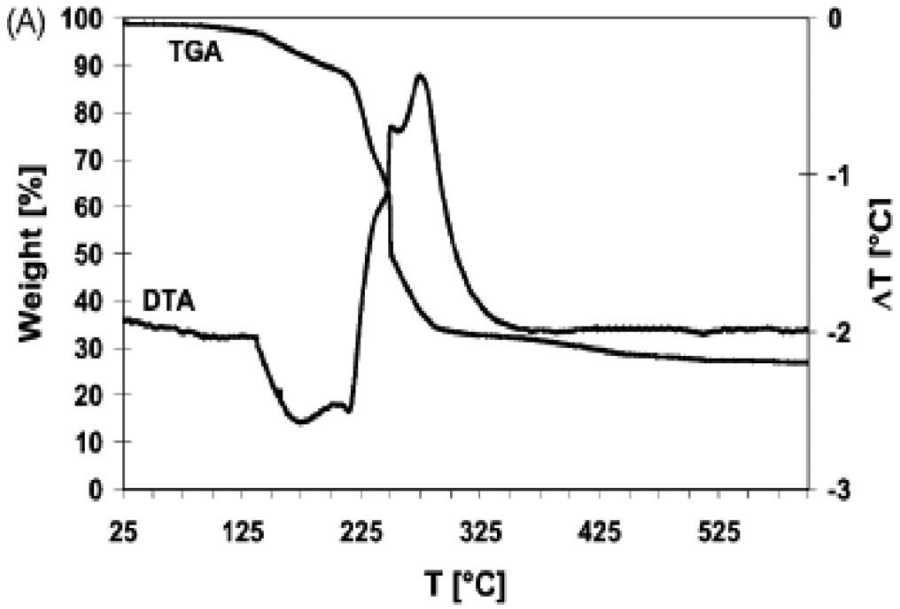

Figure 3.4 Thermograms of lanthanum nitrate-chromium nitrate-urea precursor [Biamino and Badini 2004]

3.2.4 Reactive Grinding (RG) Method

Reactive grinding is also known as high-energy mechanical synthesis or mechano-chemical synthesis. It allows attaining a pure perosvkite phase at room temperature without the thermal treatment. Mechanical impact during the process reduces the precursor's crystallite size to nano-scale [Patel and Patel 2012] while it provides a homogeneous mixture and enhances the solid state diffusion. The synthesis is performed in a closed environment without generating any waste [Quach et al. 2011, Kaliaguine et al. 2001]. The precursors with an appropriate stoichiometric ratio are mixed and ground continuously for a certain period of time in a planetary ball mill. Small balls made of YO_3 stabilized ZrO_2 and grinding jar made up of ZrO_2 are generally used in the reactive grinding method. Then the as-synthesized sample is washed with deionized water. The solid product is dried, followed by calcinations at 600◦C. After grinding, the catalyst powder is obtained [Peng et al. 2007, Wang et al. 2010]. Kaliaguine et al. [2001] synthesized a large variety of perovskites (ABO_3) by reactive grinding using the individual simple oxides of cations A and B as the reactants.

Using various grinding additives, high surface (measured after calcinations at 473 K) perovskites such as $LaCoO_3$ (>100m^2/g), $LaGaO_3$ (98.6m^2/g), $LaCo_xIn_{1-x}O_3$ (>110m^2/g), or $SrCoO_3$ (150m^2/g) are consistently prepared. The additives such as zinc oxide should be leachable. ZnO is leached out of the sample using a 2M solution of ammonium chloride. Perovskite sample prepared by the reactive grinding method display a high stability of the perovskite structure under a reducing atmosphere [Huang et al. 2007]. Figure 3.5 shows the flow diagram of reactive grinding method.

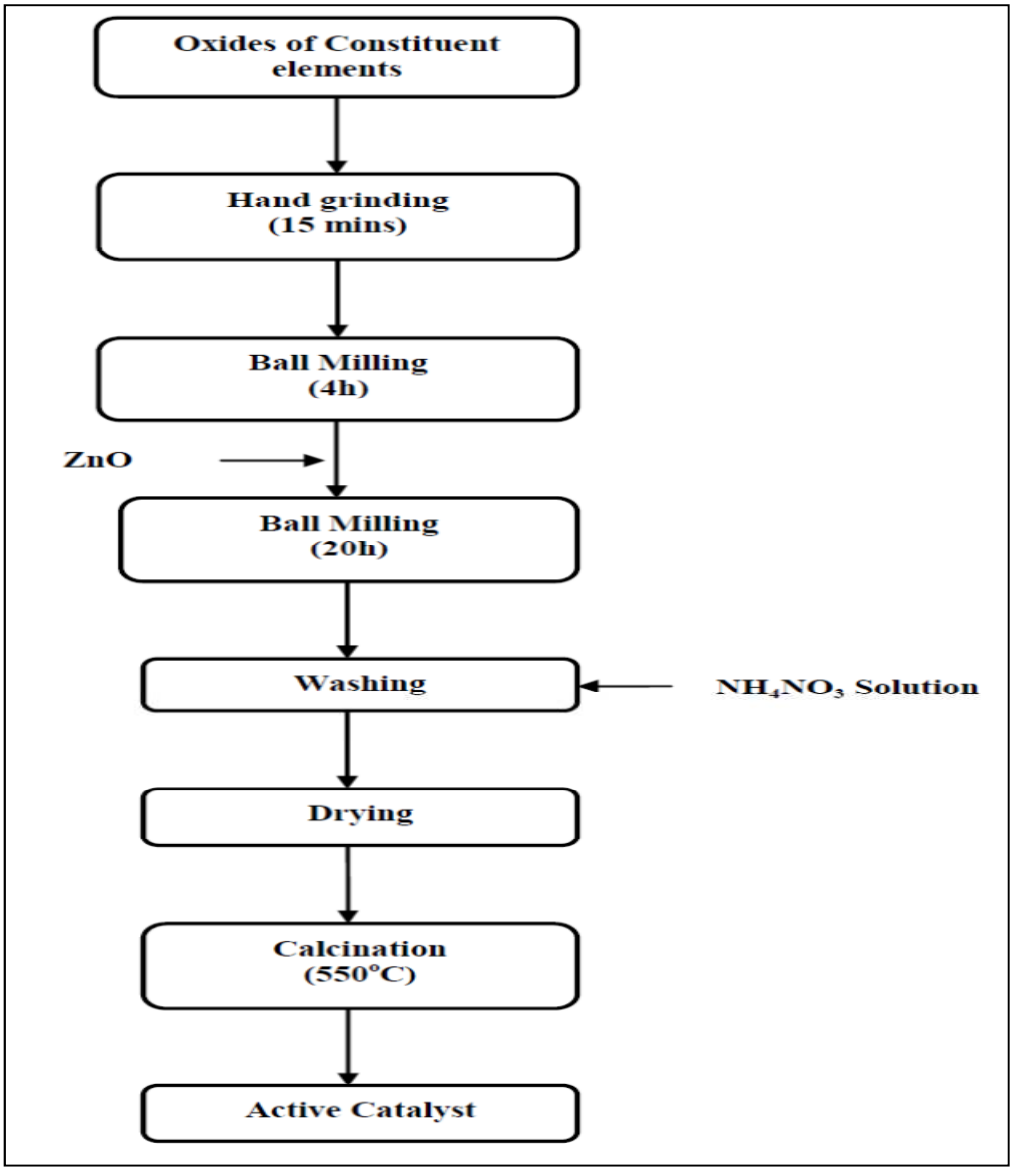

Figure 3.5 Flow diagram of Reactive Grinding Method

In the present work, a dual drive planetary ball mill shown in Fig. 3.6 (a) was used for the preparation of the catalysts. The dimensions of the jars of 67.5 mm inside diameter, outside diameter of 78 mm, height of 71.5 mm and 250 mL volume were used. The grinding balls of different diameters, 11, 9, 7 and 4mm having weight 5.78, 3.19, 1.95 and 0.43 g respectively, made of zirconia were used. The variable speed of the planetary ball mill is, 100-1500 rpm. The Jars and balls are made of zirconia and shown in figure 3.6 (b).

Figure 3.6 (a) Planetary ball mill, **(b)** Jar and grinding balls (ZrO_2)

3.3 Calcination Strategies

Calcination exposes the as prepared catalyst precursor to high temperature for the final step in the formation of finished catalysts. The primary role of calcination is to thermally decompose non-oxidic precursors, remove unwanted ligands and oxidize the support and surface species. Calcination conditions such as temperature, time and atmosphere, play dominant role in the structure and performances of the catalysts. Following calcination modes were used in the present work:

3.3.1 Calcination in Stagnant Air

This is the conventional method of calcination done in muffle furnace in air above the decomposition temperature of constituent compounds.

3.3.2 Reactive Calcination

Reactive calcinations (RC) of the precursor of perovskite catalyst were carried out by the introduction of low concentration of chemically reactive CO-air mixture (4.6% CO) at a total flow rate of 60 ml/min over the hot precursors. The RC was carried out in a down flow bench-scale tubular reactor having a definite amount of the precursor. The reactor was placed in a microprocessor temperature controlled split open furnace. The flow rates of CO and air were monitored using digital gas flow meters to feed the mixture (dried and CO_2 free) in required proportion to the reactor. The temperature of the precursor bed was measured with a thermocouple inserted in the thermo-well of the reactor reaching the bed. The temperature of the bed was increased at steady rate of heating at 2^oC/ min from room temperature to 600^oC in the flowing environment of CO-air mixture. This temperature was maintained for an hour. Then in second step of calcination temperature of the bed was increased to 750^oC and maintained for another 2h under the same atmosphere followed by cooling to room temperature. The active catalyst thus obtained was stored in an air-tight bottle.

3.4 Characterization Techniques used for Diesel Soot

The characteristics of prepared diesel soot were analysed by proximate analysis, XRD, Particle size analysis and calorimetric analysis.

3.4.1 Particle Size Analysis

The particle size analysis of the samples were measured using the Laser diffraction (Helium-Neon Laser, 5 Milli-watt maximum output) based particle size analyser (ANKERSMID, CIS-50, USA) relies on the fact that particles passing through a laser beam will scatter light at an angle that is directly related to their size. As particle size decreases, the observed scattering angle increases logarithmically. Scattering intensity is also dependent on particle size, diminishing with particle volume. Large particles therefore scatter light at narrow angles with high intensity whereas small particles scatter at wider angles but with low intensity.

3.4.2 Calorimetric Analysis

A calorimeter shown in figure 3.7 is an instrument used for measuring the caloric value of a fuel. A bomb calorimeter is a constant-volume reactor used to measure the heat of combustion of a solid or liquid fuel. Bomb calorimeter has to withstand the large pressure within the calorimeter as the reaction is being measured at high pressure. Electrical energy is used to ignite the fuel; as the fuel is burning, it heats up the bomb and surrounding water kept outside the calorimeter. The change in temperature of the water allows for calculating calorific value of the fuel.

The pelletized soot sample was tied with thread to a 10 cm length of fuse wire connected between the two electrodes and bomb assembly was tightened. The bomb was pressurized with pure oxygen at 25 atm and it was submerged under a known volume of water (ca. 1750 ml) before the charge is electrically ignited. The switch was pushed to ignite the fuse wire and thereby thread and soot pellet. Energy is released by

the combustion and heat flow crosses the stainless steel wall, thus raising the temperature of the surrounding water jacket. The temperature change in the water was then accurately measured with a temperature indicator connected to a thermo couple placed inside the calorimeter. This reading, along with a bomb factor (which is dependent on the heat capacity of the metal bomb parts), is used to calculate the energy given out by the sample burn. A small correction is made to account for the electrical energy input as the burning of fuse wire and thread. After the temperature rise has been measured, the excess pressure in the bomb is released.

Figure 3.7 General view of the Bomb Calorimeter

Since, there is no heat exchange between the calorimeter and surroundings → Q = 0 (adiabatic); no work performed → W = 0. Thus,

The total internal energy change ΔU (total) = Q + W = 0

Also, total internal energy change ΔU (total) = ΔU (system) + ΔU (surroundings) = 0

ΔU (system) = - ΔU (surroundings) = -Cv ΔT (constant volume → dV = 0)

Where Cv = heat capacity of the bomb

Before the bomb can be used to determine heat of combustion of any compound, it must be calibrated. The value of Cv can be estimated by

Cv (calorimeter) = m (water). Cv (water) + m (steel). Cv (steel)

m (water) and m (steel) can be measured;

Cv(water)= 1 cal/g.K

Cv(steel)= 0.1 cal/g.K

In laboratory, Cv is determined by running a compound with known heat of combustion value: Cv = Hc/ΔT

Common compounds are benzoic acid (Hc = 6318 cal/g) or p-methyl benzoic acid (Hc = 6957 cal/g).

Temperature (T) is recorded every minute and ΔT = T (final) - T (initial)

A small factor contributes to the correction of the total heat of combustion is the fuse wire. Nickel fuse wire is often used and has heat of combustion = 981.3 cal/g. In order to calibrate the bomb, a small amount (~ 1 g) of benzoic acid or p-methyl benzoic acid is weighed. A length of Nickel fuse wire (~10 cm) is weighed both before and after the combustion process. Mass of fuse wire burned Δm = m (before) - m (after)

The combustion of sample (benzoic acid) inside the bomb,

ΔHc = ΔHc (benzoic acid) x m (benzoic acid) + ΔHc (Ni fuse wire) x Δm (Ni fuse wire)

ΔHc = Cv. ΔT; Cv = ΔHc/ΔT

Once, Cv value of the bomb is determined, the bomb is ready to use to calculate heat of combustion of any compounds by ΔHc = Cv. ΔT.

3.4.3 Proximate Analysis

Proximate analysis of soot was done for the moisture, volatile matter (VM), ash and fixed carbon content of the soot. For the determination of moisture, soot was heated at 108^{o}C for 1h with lids of the silica crucible open. Volatile matter was determined by heating soot at 925^{o}C for 7min in absence of air (lid close). Ash was determined by two step heating: i) heating soot at 425^{o}C for 30min in absence of air and ii) heating at 775^{o}C in presence of air. Lastly fixed carbon was calculated by subtracting moisture, VM and ash from total weight.

3.5 Characterization Techniques used for Catalysts

The information on the structure of the catalysts provides insight into the inter-relation between the parameters of catalysts preparation and the performance of the catalyst. The catalyst characterization, i.e. the investigation of relevant aspects of the catalyst structure may also be required for quality control on the basis of previous empirical observations. The information based on characterization of the catalyst is useful for catalytic process optimization and for the manufacture of catalyst. The characterization helps to understand the inter-relationship between the activity and selectivity of a catalyst and its different physical and chemical properties. The prepared catalysts were characterized by various techniques like X-ray diffraction (XRD) analysis, Fourier Transform Infrared Spectrum (FTIR), Scanning electron microscopy (SEM) and low temperature N_2 adsorption as given in Table 3.1.

Table 3.1 Techniques used for characterization of catalyst

Techniques Applied	Physico-Chemical Properties
Low temperature N_2-sorption	Textural properties: surface area, pore volume, pore size distribution, average pore diameter
Fourier transform infrared spectroscopy (FTIR)	Infrared spectrum of absorption, emission, and photoconductivity
X-ray photoelectron spectroscopy (XPS)	Elemental composition, empirical formula, chemical state
Scanning electron microscopy (SEM)	Surface structure (texture), particle size estimation,
Energy-dispersive X-ray spectroscopy (EDX)	Elemental analysis, Chemical characterization
X ray diffraction (XRD)	Phase analysis, mean crystallite size, crystal size, crystal size distribution and lattice parameter

3.5.1 Textural Characterization by N_2-Physisorption

The standard method for measuring specific surface area is by gas adsorption and the application of the Brunauer, Emmett, and Teller (BET) equation [Brunauer et al. 1938] which is described in detail in a number of reference books [Gregg and Sing, 1982, Condon 2006]. BJH analysis can also be employed to determine pore area and specific pore volume using adsorption and desorption techniques. This technique characterizes pore size distribution independent of external area due to particle size of the sample. The parameters like surface area, distribution of the sizes of pores and particles and pore shapes play a major role in governing the vital reaction parameters like catalytic activity, selectivity and stability as well as physical factors such as permeability, diffusivity, effectiveness factor and mechanical strength.

Principle of BET analysis: The principle of BET analysis is that at low relative pressure, gas adsorbs to a solid in a monolayer (multilayers form at higher pressures). By knowing the number of gas molecules in a monolayer and the dimensions of an individual molecule, the surface area covered by the monolayer can be calculated. The

BET equation (Smith 1970) models a measured number of moles of adsorbate (n) adsorbed on 1 g of sample with the applied gas pressure (P) following the relationship given in equation 3.4.

$$\frac{\boldsymbol{P/P_o}}{\boldsymbol{n(1-\frac{P}{P_o})}} = \frac{\boldsymbol{1}}{\boldsymbol{n_m c}} + \frac{\boldsymbol{c-1}}{\boldsymbol{n_m c}}\left(\frac{\boldsymbol{P}}{\boldsymbol{P_o}}\right) \qquad (3.4)$$

Where;

n_m = calculated number of moles adsorbed as a monolayer on 1 g of adsorbent,

P = gas pressure,

P_o = saturation vapor pressure of the gas, and

c = a constant that is dependent upon the shape of the isotherm.

n_m is obtained by plotting $P/V_a(P_o - P)$ against P/P_o, where V_a α n, is the volume of gas adsorbed per gram of sample normalized to standard temperature and pressure (STP) (mL/g). Generally the plot is linear at low relative pressures (P/P_o< 0.3). The slope of the linear part of the graph has a slope, s = $(c - 1)/V_m c$ and an intercept, i = $1/V_m c$, where V_m α n_m, is the volume of gas required to form a monolayer on a unit gram of the sample (mL/g). Both s and i have units of cm^3/g at STP. By algebraic substitution, $V_m = (s + i)^{-1}$. Finally, the BET specific surface area (SSA) can be calculated using equation 3.5.

$$\boldsymbol{SSA} = \frac{\boldsymbol{LV_m a_m}}{\boldsymbol{V_l}} \qquad (3.5)$$

Where;

a_m = Effective area occupied by a molecule of the N_2 adsorbate (16.2×10^{-20} m^2 for N_2),

L = Avogadro's number ($6.02 * 10^{23}$ molecules/moles)

V_1 = molar volume of the analysis gas (22.4 L for N_2) at STP.

Substituting these values in equation 3.5 the surface area per gram is given by equation 3.6.

$$\textbf{SSA= 4.35 } V_m \textbf{ m}^2\textbf{/g solid adsorbent} \qquad (3.6)$$

Brunauer-Emmett-Teller (BET) surface areas of the catalyst samples were measured at -196^{o}C using a Micromeritics ASAP 2020 Analyser in present case. Samples were degassed at 300^{o}C under vacuum prior to the measurement. The calculation of SSA was performed using the adsorption data in the relative pressure (p/p_o) range from 0.05 to 0.35, and the total pore volume were determined from the amounts adsorbed at p/p_o = 0.99. The pore size distribution curve was calculated based on the desorption curve of the isotherm using the Barrett-Joyner-Halenda (BJH) algorithm. The pore diameter was defined as the position of the maximum in the pore-size distribution.

3.5.2 Spectral Characterization by FTIR and XPS

FTIR and XPS instruments were used for spectral characterization of the catalyst samples.

(i) FTIR Spectrometer

Infrared spectroscopy has been a workhorse technique for materials analysis. An infrared spectrum represents a fingerprint of a sample with absorption peaks which correspond to the frequencies of vibrations between the bonds of the atoms making up the material. Because each different material is a unique combination of atoms, no two compounds produce the exact same infrared spectrum. Therefore, infrared spectroscopy can result in a positive identification (qualitative analysis) of every different kind of material. In addition, the size of the peaks in the spectrum is a direct indication of the amount of material present. With modern software algorithms, infrared is an excellent

tool for quantitative analysis. It can identify unknown materials and determine the quality or consistency of a sample.

Principle of FTIR: In FTIR, a single optical device called interferometer is used. Most interferometers are employing a beam splitter which takes the incoming infrared beam and divides it into two optical beams. One beam reflects off of a flat mirror which is fixed in place. The other beam reflects off of a flat mirror which is on a mechanism that allows this mirror to move a very short distance (typically a few millimetres) away from the beam splitter. The two beams reflect off of their respective mirrors and are recombined when they meet back at the beam splitter. Because the path that one beam travels is a fixed length and the other is constantly changing as its mirror moves, the signal which exits the interferometer is the result of these two beams "interfering" with each other. The resulting signal is called an interferogram which has the unique property that every data point (a function of the moving mirror position) which makes up the signal has information about every infrared frequency which comes from the source**.**

Here, FTIR spectra were recorded in the range of 400-4000 cm^{-1} on Shimadzu 8400 FTIR spectrometer with KBr pellets. The infrared spectra were recorded at room temperature of the samples.

(ii) X-ray Photoelectron Spectroscopy (XPS)

XPS is a quantitative spectroscopic technique that measures the elemental composition of the surface, empirical formula of pure materials, chemical state and electronic state of the elements that exist within the material, elements that contaminate a surface, uniformity of elemental composition across top surface.

Principle of XPS: It is an electron spectroscopic method that uses X-rays to eject electrons from inner-shell orbitals. The kinetic energy, E_k, of these photoelectrons is

determined by the energy of X-ray radiation, h_v, and the electron binding energy, E_b, as given by equation (3.7).

$$\mathbf{E_k = h\nu - E_b} \qquad (3.7)$$

The experimentally measured energies of the photoelectrons are given by equation (3.8).

$$\mathbf{E_k = h\nu - E_b - E_w} \qquad (3.8).$$

Where E_w is the work function of the spectrometer.

The electron binding energies are dependent on the chemical environment of the atom, making XPS useful to identify the oxidation state and ligands of an atom. Ejected electrons can escape only from a depth of approximately 3 nm or less, making electron spectroscopy most useful to study surfaces of solid materials. In present work, XPS was performed on an Amicus spectrometer equipped with Mg Kα X-ray radiation. For typical analysis, the source was operated at a voltage of 15 kV and current of 12 mA. Pressure in the analysis chamber was less than 10^{-5} Pa. The binding energy scale was calibrated by setting the main C 1s line of adventitious impurities at 284.7 eV, giving an uncertainty in peak positions of ±0.2 eV.

3.5.3 Morphological Characterization by SEM-EDX

Morphological characterization was performed by using scanning electron microscopy (SEM). SEM is used to estimate the average aggregate size, crystallinity degree of the oxides and the microstructures of the powders. SEM analysis is considered as "non-destructive"; i.e. x-rays generated by electron interactions do not lead to volume loss of the sample, so it is possible to analyze the same materials repeatedly. Topographical images in a SEM are formed from back-scattered primary or low-energy secondary electrons. The best resolution is about 2-5 nm but many routine studies are satisfied with a lower value and exploit the case of image interpretation and the extrordinary

depth of field to obtain a comprehensive view of the spccimen. With non-crystalline catalysts, SEM is especially useful for examining the distribution and sizes of mesopores.

Principle of SEM: In the SEM, electrons from the electron gun are focused to a small spot, 50-100Å in diameter, on the surface of the sample. Electron beams which have been accelerated through a voltage in between 1 and 50 kV, are used for most applications. Accelerated electrons in an SEM carry significant amounts of kinetic energy, and this energy is dissipated as a variety of signals produced by electron-sample interactions when the incident electrons are decelerated in the solid sample. These signals include secondary electrons (that produce SEM images), back-scattered electrons (BSE), diffracted back-scattered electrons (EBSD that are used to determine crystal structures), photons (characteristic X-rays that are used for elemental analysis and continuum X-rays), visible light and heat. Secondary electrons and backs-cattered electrons are commonly used for imaging samples. Secondary electrons are most valuable for showing morphology and topography on samples and back-scattered electrons are most valuable for illustrating contrasts in composition in multiphase samples (i.e. for rapid phase discrimination).

Energy-dispersive X-ray spectroscopy (EDX), sometimes called energy dispersive X-ray analysis (EDXA) or energy dispersive X-ray microanalysis (EDXMA), is an analytical technique used for the elemental analysis or chemical characterization of a sample.

Principle of EDX: It relies on an interaction of some source of X-ray excitation and a sample. Its characterization capabilities are due in large part to the fundamental principle that each element has a unique atomic structure allowing unique set of peaks on its X-ray emission spectrum [Goldstein 2003]. To stimulate the emission of

characteristic X-rays from a specimen, a high-energy beam of charged particles such as electrons or protons (see PIXE), or a beam of X-rays, is focused into the sample being studied. At rest, an atom within the sample contains ground state (or unexcited) electrons in discrete energy levels or electron shells bound to the nucleus. The incident beam may excite an electron in an inner shell, ejecting it from the shell while creating an electron hole where the electron was present. An electron from an outer, higher-energy shell then fills the hole, and the difference in energy between the higher-energy shell and the lower energy shell may be released in the form of an X-ray. The number and energy of the X-rays emitted from a specimen can be measured by an energy-dispersive spectrometer. As the energies of the X-rays are characteristic of the difference in energy between the two shells and of the atomic structure of the emitting element, EDS allows the elemental composition of the specimen to be measured [Goldstein 2003]. In present study, the surface morphology was determined with FEI Quanta 200 SEM instrument as well as Zeiss EVO 18 SEM-EDX instrument. An accelarating voltage of 30kV was applied. Micrographs were recorded at 10000 and 20000x magnification.

3.5.4 X-Ray Diffraction Analysis

X-ray diffraction is the most widely used and the least ambiguous method for the precise determination of the positions of atoms in all kinds of matter ranging from fluids and powders to perfect crystals. It is a non-destructive technique applied for the characterization of crystalline materials. It provides information about the structure, phases, preferred crystal orientation and other structural parameters such as lattice parameters, crystallite size, crystallite, and strain and crystal defects.

Principle of X-ray Diffraction: X-rays are electromagnetic radiation of exactly the same nature as light but of very much shorter wavelength lying approximately in the

range 0.5-2.5 Å. X-rays interact with electrons in matter. Matter absorbs X-rays in two distinct ways, by scattering and by true absorption. When a beam of X-rays impinges on the material it is scattered in various directions by the electron cloud of the atoms. If the wave length of X-rays is comparable to the separation between the atoms then interference can occur. X-ray diffraction peaks are produced by constructive interference of monochromatic light scattered by each set of lattice plans at specific angles. The peak intensities are determined by the atomic decoration in the lattice plans. For an ordered arrays of scattering centres (such as atoms or ions in a crystalline solid), this can give rise to interference maxima and minima. In this study, the analyses of the samples were carried out using a Rigaku Ultima IV X-ray diffractometer operating at 40mA and 40kV using CuKα1 radiation source (λ = 1.5405 Å). The data of 2θ from 0^o to 80^o were collected with a step size of 0.02. The patterns were compared with JCPDS reference data for phase identification. The Scherrer equation (equation 3.9) was used to calculate the crystallite size of the prepared samples is as follows:

$$\boldsymbol{d = \frac{0.89\lambda}{\beta cos\theta}} \qquad (3.9)$$

Where; d, λ, θ and β are the crystallite size, X-ray wavelength (1.518 Å), Bragg diffraction angle and full width at the half maximum (FWHM) of the diffraction peak respectively.

3.6 Catalytic Activity Test

3.6.1 Soot-Catalyst Contacts

The catalytic oxidation of soot was studied under tight contact and loose contact by following mixing procedures:

(i) Tight Contact

For tight contact the soot-catalyst mixture, in an appropriate ratio, was milled in an agate mortar for 15 min.

(ii) Loose Contact

The soot-catalyst mixture, in an appropriate ratio, was mixed with a spatula for "loose contact". Loose contact mode represents near real contact of soot and catalyst in a DPF.

3.6.2 Experimental Set-up

The experimental setup used for the catalytic activity measurement in the present study is shown in Figure 3.8. It can be divided into following three sections:

i) Air feeding section,
ii) Reaction section, and
iii) Product analysis section.

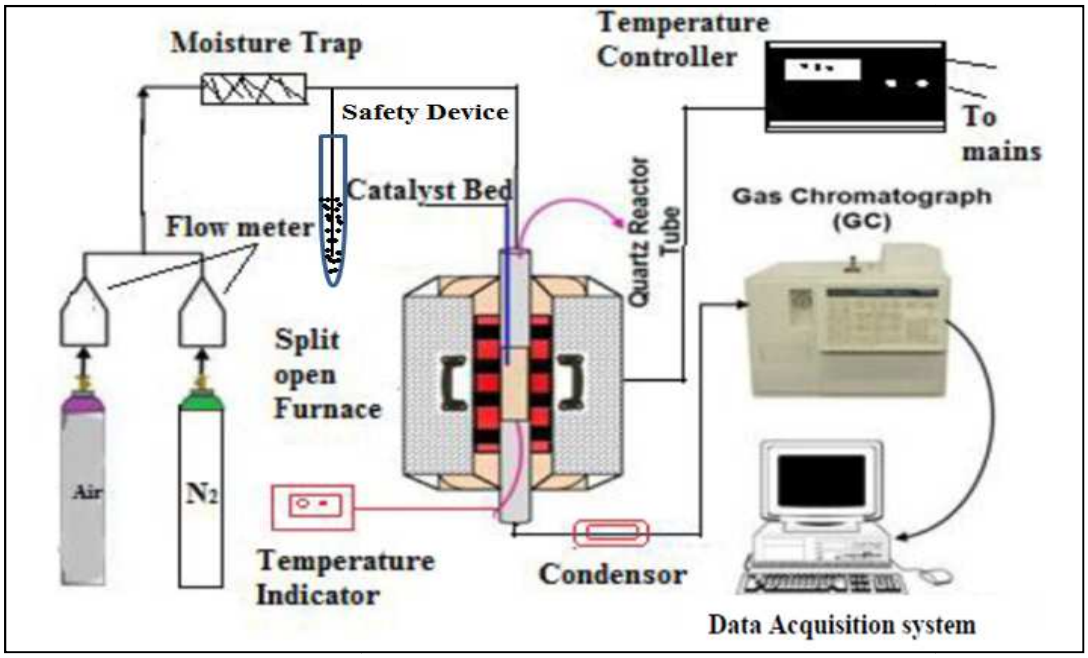

Figure 3.8 Schematic diagram of Experimental Setup

(i) Air feeding section

Air from compressed cylinder was fed to the reactor, after purifying free from moisture and CO_2 by passing through a tower packed with CaO and KOH pellets. The air was

monitored with the help of a digital gas flow meter. A safety device in the form of mercury sealing was provided in the feeding line to check any pressure build up.

(ii) Reaction section

The catalytic performance of the prepared catalyst for oxidation of soot was evaluated in a compact fixed bed tubular quartz reactor shown in figure 3.9. The reactor was consisting of two co-axial tubes of 20mm and 50mm diameter. A helical coil of quartz tube in between the co-axial tubes served as a pre-heater of the air. There is a hole in the lower part of the outer tube, to take care of breakage due to the expansion or contraction of air in between co-axial tubes as the unit is subjected to the variation of temperature from ambient to the reaction temperature. The pre-heated air enters the catalyst bed, kept in the inner tube as shown in the figure. The product stream from the bottom of the reactor is cooled in a condenser to the ambient temperature and then analysed with the help of an online Gas chromatograph.

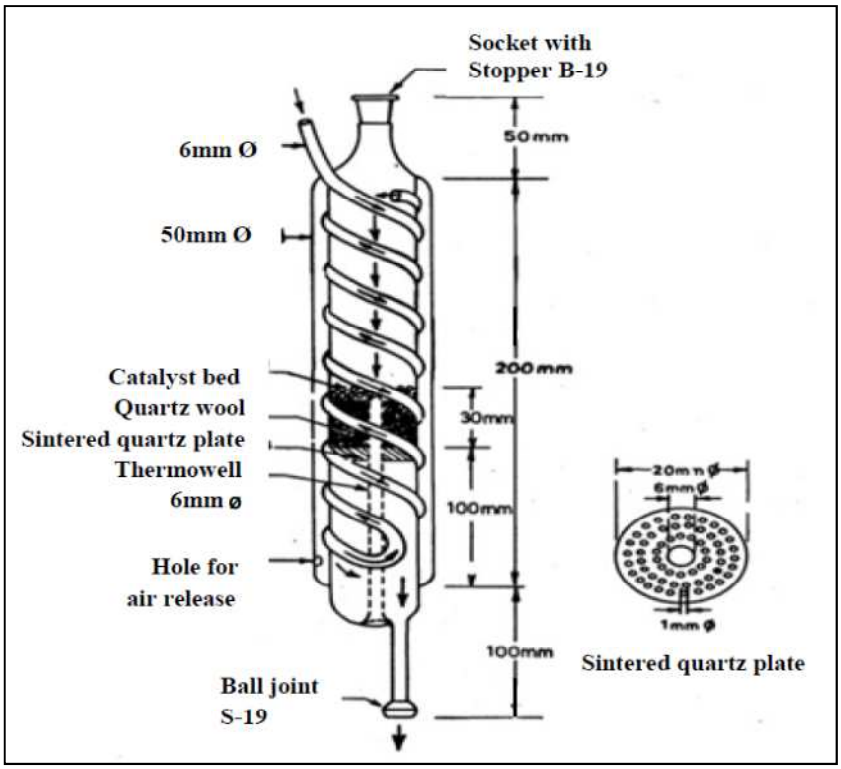

Figure 3.9 Schematic diagram of the Reactor

The reactor was mounted vertically in a split open furnace. The down flow stream of air was used to avoid any distortion of the bed. The soot-catalyst (catalyst bed diameter 20mm and height 1.27 mm) was placed on a thin layer of quartz wool which is supported on perforated quartz disc inside the inner tube. A thermocouple-well made of 4mm diameter tube was inserted axially from the bottom all the way to the centre of the disc for temperature measurement and control. The catalytic activity was evaluated by placing in the reactor a mixture of 110 mg catalyst-soot (1/10 wt. ratio) under tight/loose contact and the air oxidation was carried out in the temperature range from ambient to total conversion of soot at a constant heating rate of $1^{o}C\ min^{-1}$. The inlet air free from moisture and CO_2 was fed to the reactor with a steady flow rate of 150 ml min^{-1}. The General view of the experiment assembly is shown in figure 3.10.

Figure 3.10 General view of the Experiment Assembly

(iii) Product Analysis Section

The reactor outlet cooled gases were analysed for CO and CO_2 by an on-line gas chromatograph (nucon 5765) equipped with methanizer using a porapak Q-column and FID detector; maintaining oven, injector and detector temperatures at 60, 80 and 80 ^{o}C respectively.

Figure 3.11 General view of the Gas Chromatograph

3.6.3 Gas Chromatograph (GC)

A gas chromatograph (GC) is an analytical instrument that measures the content of various components in a sample. The analysis performed by a gas chromatograph is called gas chromatography.

Principle of gas chromatography: The sample solution injected into the instrument enters a gas stream which transports the sample into a separation tube known as the "column." (Helium or nitrogen is used as the so-called carrier gas). The various components are separated inside the column. The detector measures the quantity of the components that exit the column. To measure a sample with an unknown concentration, a standard sample with known concentration is injected into the instrument. The

standard sample peak retention time (appearance time) and area are compared to the test sample to calculate the concentration. In the present work 5765 Nucon Gas Chromatograph was used as shown in Figure 3.11 and the schematic diagram of the GC is shown in figure 3.12.

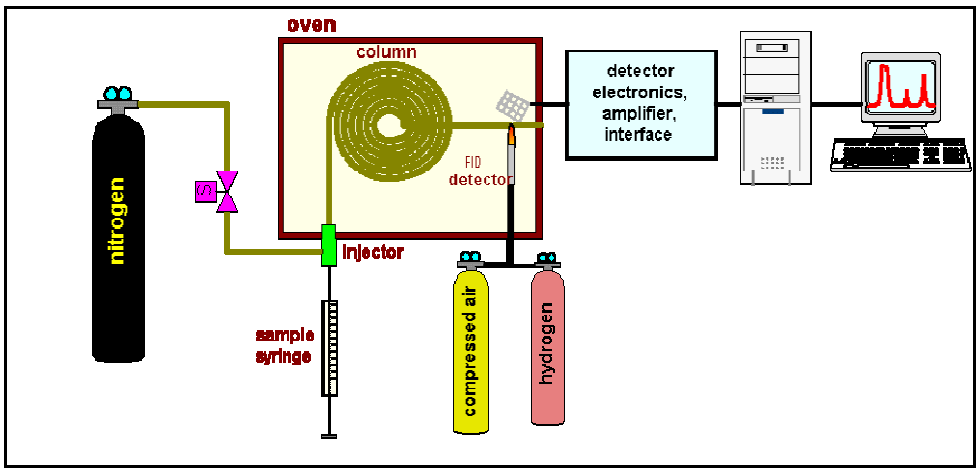

Figure 3.12 Schematic diagram of Gas Chromatograph

Various instrumental components used in GC are mentioned below:

Carrier gas: The carrier gas must be chemically inert. Commonly used gases include nitrogen, helium, argon, and carbon dioxide. The choice of carrier gas is often dependent upon the type of detector which is used.

Sample injection port: For optimum column efficiency, the sample should not be too large, and should be introduced onto the column as a "plug" of vapors - slow injection of large samples causes band broadening and loss of resolution. The most common injection method is where a micro syringe is used to inject sample through a rubber septum into a flash vaporizer port at the head of the column. The temperature of the sample port is usually about 50°C higher than the boiling point of the least volatile component of the sample. For packed columns, sample size ranges from tenths of a micro liter up to 20 micro liters. Capillary columns, on the other hand, need much less

sample, typically around 10^{-3} m. For capillary GC, split/split less injection is used as shown in Figure 3.13.

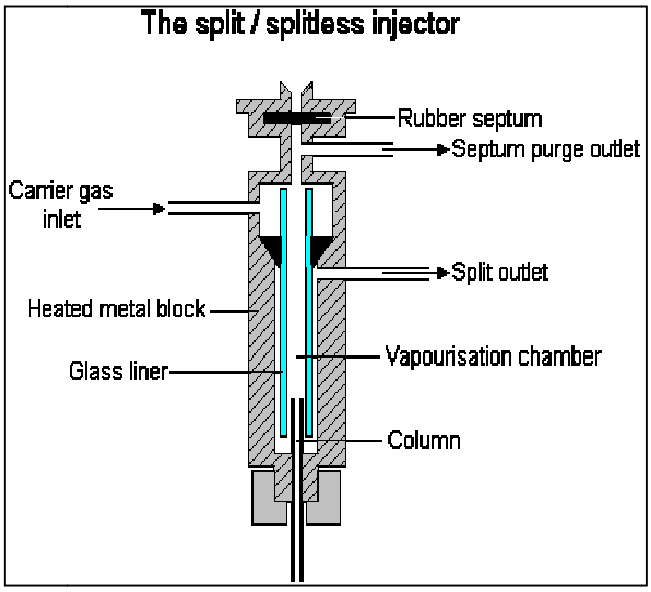

Figure 3.13 Injector diagram for Gas Chromatograph

The injector can be used in one of two modes; split or split less. The injector contains a heated chamber containing a glass liner into which the sample is injected through the septum. The carrier gas enters the chamber and can leave by three routes (when the injector is in split mode). The sample vaporizes to form a mixture of carrier gas, vaporized solvent and vaporized solutes. A proportion of this mixture passes onto the column, but most exits through the split outlet. The septum purge outlet prevents septum bleed components from entering the column.

Columns: For precise work, column temperature must be controlled to within tenths of a degree. The optimum column temperature is dependent upon the boiling point of the sample. As a rule of thumb, a temperature slightly above the average boiling point of the sample results in an elution time of 2-30 minutes. Minimal temperatures give good resolution, but increase elution times. If a sample has a wide boiling range, then temperature programming can be useful. The column temperature is increased (either continuously or in steps) as separation proceeds.

Detectors: The most commonly used detectors are the flame ionization detector (FID) and the thermal conductivity detector (TCD). Both are sensitive to a wide range of components, and both work over a wide range of concentrations. While TCDs are essentially universal and can be used to detect any component other than the carrier gas (as long as their thermal conductivities are different from that of the carrier gas, at detector temperature), FIDs are sensitive primarily to hydrocarbons, and are more sensitive to them than TCD. However, a FID cannot detect water. Both detectors are also quite robust. Since TCD is non-destructive, it can be operated in-series before a FID (destructive), thus providing complementary detection of the same analytes.

Thermal Conductivity Detector (TCD)

This common detector relies on the thermal conductivity of matter passing around tungsten -rhenium filament with a current traveling through it [Harris 1999]. In this set up helium or nitrogen serve as the carrier gas because of their relatively high thermal conductivity which keep the filament cool and maintain uniform resistivity and electrical efficiency of the filament. However, when analyte molecules elute from the column, mixed with carrier gas, the thermal conductivity decreases and this causes a detector response [Higson 2004]. The response is due to the decreased thermal conductivity causing an increase in filament temperature and resistivity resulting in fluctuations in voltage. Detector sensitivity is proportional to filament current while it is inversely proportional to the immediate environmental temperature of that detector as well as flow rate of the carrier gas.

Flame Ionization detector (FID)

In this common detector electrodes are placed adjacent to a flame fueled by hydrogen / air near the exit of the column, and when carbon containing compounds exit the column they are pyrolyzed by the flame [Higson 2004]. This detector works only for organic /

hydrocarbon containing compounds due to the ability of the carbons to form cations and electrons upon pyrolysis which generates a current between the electrodes. The increase in current is translated and appears as a peak in a chromatogram. FIDs have low detection limits (a few picograms per second) but they are unable to generate ions from carbonyl containing carbons [Harris 1999]. FID compatible carrier gasses include nitrogen, helium, and argon. Figure 3.14 shows the schematic diagram of the Flame ionization detector.

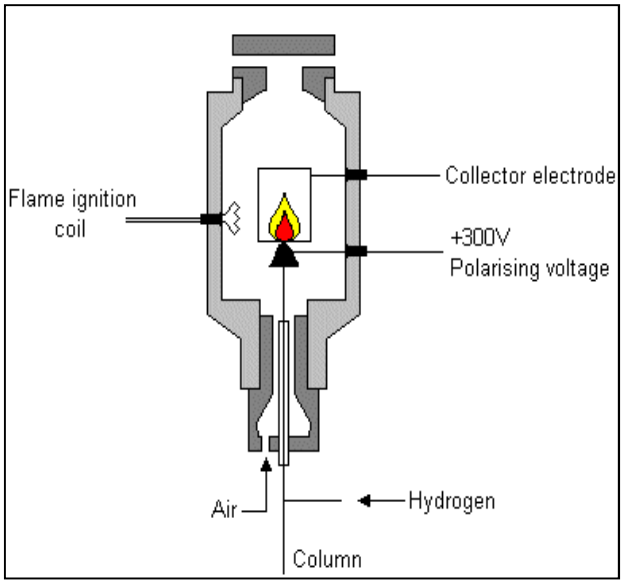

Figure 3.14 Schematic diagram of the Flame Ionization Detector.

In the GC analysis there comes a term called retention time (RT). The RT comes early (shorter) for single molecule compound, and longer for complex one. The RT is the time it takes for a compound to travel from the injection port to the detector; it is reported in minutes on our GC. Because it has to be ones adsorbed and again desorbed. There are different peaks for different compounds.

3.6.4 Calculation of the soot conversion

A graph between chromatogram areas for CO_2 vs. increasing temperature for catalytic soot oxidation was plotted as shown in figure 3.15 for a typical experimental run. The fractional conversion of soot, (X_i) is defined as (equation 3.10):

$$\mathbf{X_i = (M_o - M_i)/M_o} \qquad (3.10)$$

Where, M_o is the weight of initial soot taken and M_i is the weight of soot at temperature T_i. M_o is proportional to total area of the graph bounded between temperature of initiation of soot oxidation (T_o) and temperature for 100% oxidation of soot (T_f), can be given as (equation 3.11)

$$\mathbf{M_o\ \alpha\ \sum_{To}^{Tf}(\Delta \bar{A}_{CO2})_i \Delta T_i} \qquad (3.11)$$

M is the weight of soot at a typical temperature (T_i), higher than the temperature (T_o). The weight loss (M_o-M_i) at temperature T_i, which is proportional to the area bounded by the graph between T_o and T_i, can be given as (equation 3.12)

$$\mathbf{(M_o\text{-}Mi)\ \alpha\ \sum_{To}^{Ti}(\Delta \bar{A}_{CO2})_i \Delta T_i} \qquad (3.12)$$

Therefore, the value of X at various extent of reaction can be calculated using the following formula (equation 3.13):

$$\boldsymbol{X_i} = \frac{\mathbf{M_o - M_i}}{\mathbf{M_o}} = \frac{\sum_{T_o}^{T_i}(\Delta \bar{A}_{CO2})_i \Delta T_i}{\sum_{T_o}^{T_i}(\Delta \bar{A}_{CO2})_i \Delta T_i} \qquad (3.13)$$

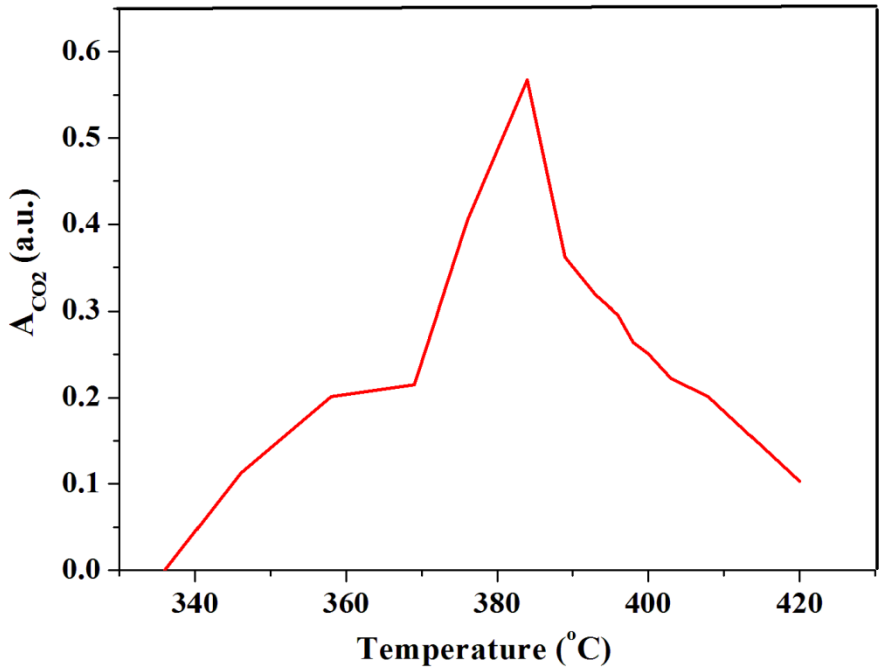

Figure 3.15 A typical plot of chromatogram area of CO_2 formed by soot oxidation vs. Temperature

Thus, the above graph (figure 3.15) can also be plotted between conversion vs. temperature shown in figure 3.16.

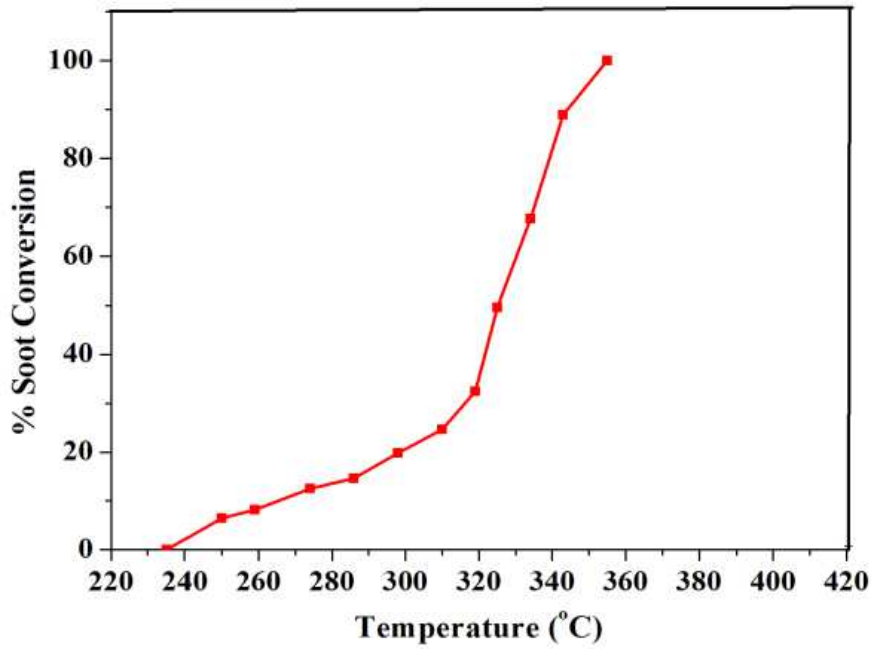

Figure 3.16 A typical plot of Soot conversion vs. Temperature